

DYNAMICS MODELLING OF A PARALLEL FLIGHT SIMULATOR

STEFAN STAICU , CONSTANTIN OCNARESCU, LIVIU UNGUREANU

Abstract. Recursive matrix relations for dynamics analysis of a parallel manipulator, namely the spatial flight simulator, is established in this paper. Knowing the general motion of the platform, the inverse dynamics problem is solved using an approach based on explicit equations of parallel robots dynamics. Finally, some simulation graphs for the input forces and powers are obtained.

Key words: connectivity relations, dynamics, flight simulator, parallel robot.

1. INTRODUCTION

Parallel robots are closed-loop structures presenting very good potential in terms of accuracy, stiffness and ability to manipulate large loads. One of the main bodies of the mechanism is fixed and is called *the base*, while the other is regarded as movable and hence is called *the moving platform* of the manipulator. The links of the robot are connected one to the other by spherical joints, universal joints, revolute joints or prismatic joints. Generally, the number of actuators is typically equal to the number of degrees of freedom and each leg is controlled at or near the fixed base [1–3].

These mechanisms can be found in practical applications, in which it is desired to orient a rigid body in space of high speed, such as flight simulators [4–6] and positional trackers [7,8]. A first spatial robot used in the amusement parks was built in 1928 by James E. Gwinnett [9] and was patented as a simulator by Galanov and Diaciun [10].

In the present paper, a recursive matrix method is applied to the inverse dynamics analysis of a spatial 3-DOF parallel mechanism, to prove that the number of equations and computational operations reduces significantly by using a set of matrices for dynamics modelling.

“Politehnica” University of Bucharest, Department of Mechanics, Department of Mechanisms Theory and Robotics, Romania

Rom. J. Techn. Sci. – Appl. Mechanics, Vol. 58, N° 3, P. 273–285, Bucharest, 2013

2. KINEMATICS ANALYSIS

With a closed-loop structure, the parallel manipulator has a spatial construction and is used as a flying simulator in the amusement parks. Additionally, a closed cab with two doors is placed on the moving platform (Fig. 1).

The architecture of the robot consists of a fixed triangular base $A_1B_1C_1$ and an upper moving platform $A_4GB_4C_4$ that is a rectangle with b and h the lengths of the geometric characteristics, two passive legs and three active extensible legs. The first active leg A is typically contained within the Ox_0y_0 median vertical plane of the cab platform, whereas the remaining active legs B, C are starting from a perpendicular vertical plane, symmetrically placed relative to the median plane. Provided with identical kinematical structure, these last active limbs connect the fixed base to the moving platform by two universal (U) joints interconnected through a prismatic (P) joint made up of a cylinder and a piston. Hydraulic or pneumatic systems can be used to vary the lengths of the prismatic joints and to control the location of the platform. There are three active prismatic joints A_2, B_3, C_3 , four passive universal joints B_1, B_4, C_1, C_4 , seven passive revolute joints $A_1, A_3, A_4, D_1, D_2, E_1, E_2$ and one internal passive prismatic pair jointed at the point E_2 .

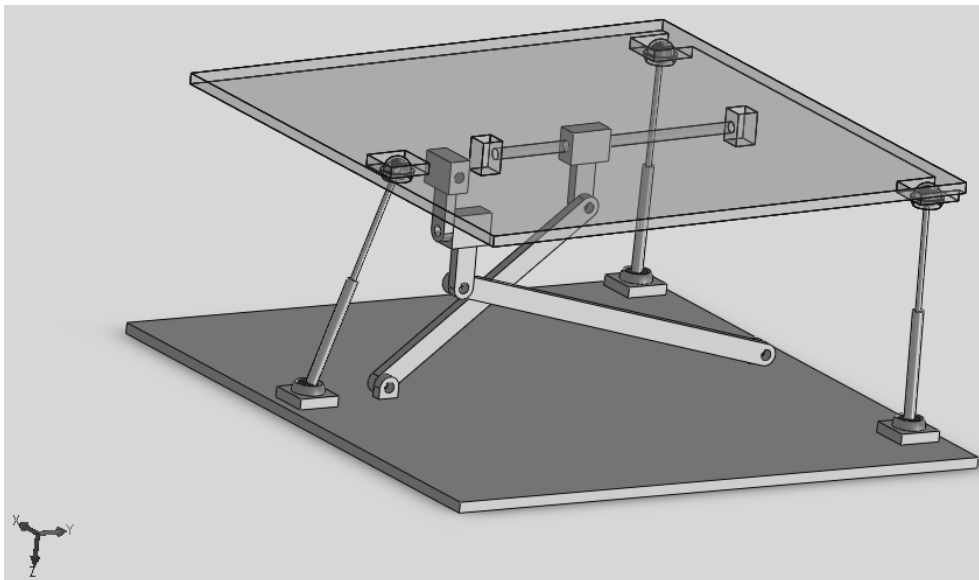


Fig. 1 – Parallel flight simulator.

For the purpose of analysis, we assign a fixed Cartesian coordinate system $Ox_0y_0z_0(T_0)$ at the point O of the fixed base platform and a mobile frame $Gx_Gy_Gz_G$ attached on the mobile platform at its characteristic point G . Grübler mobility equation predicts that the device has certainly three degrees of freedom.

The moving platform is initially located at a *central configuration*, where the platform is not rotated with respect to the fixed base and the point G is located at an elevation h_G . We also consider that the three sliders A_2, B_3, C_3 are initially starting from the positions $A_1A_2 = s_A, B_2B_3 = s_B, C_2C_3 = s_C$ (Fig. 2).

To simplify the graphical image of the kinematical scheme of the mechanism, in what follows we will represent the intermediate reference systems by only two axes, so as is used in most of robotics papers [1, 2, 11]. It is noted that the relative rotation with angle $\varphi_{k,k-1}$ or the relative translation of the body T_k with the displacement $\lambda_{k,k-1}$ must always be pointed along the direction of the z_k axis.

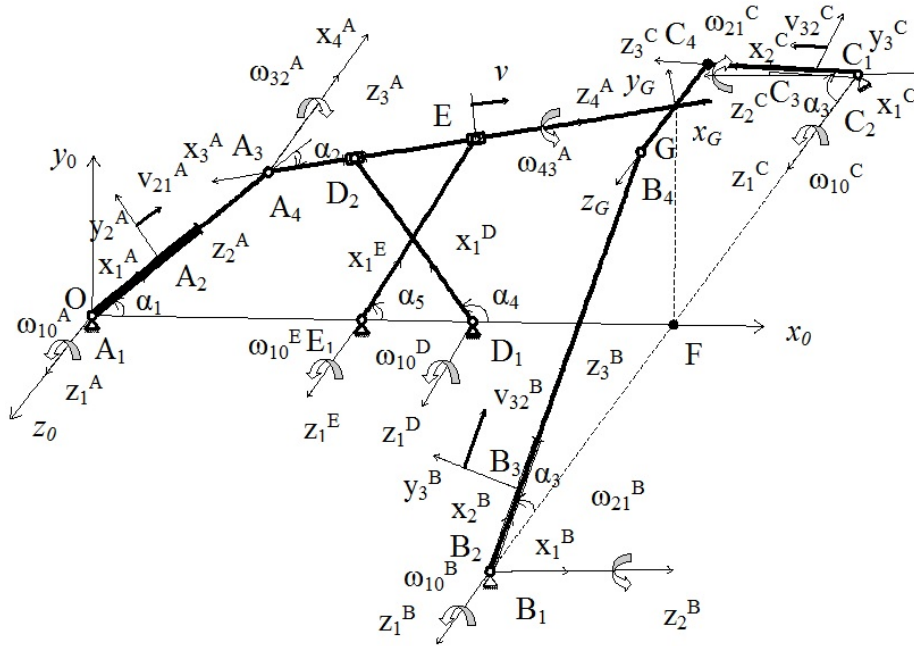


Fig. 2 – Kinematical scheme of parallel mechanism.

The leg A consists of a fixed revolute joint, a moving cylinder of length l_1 , mass m_1^A and tensor of inertia \hat{J}_1^A , which has a rotation about z_1^A axis with the angle φ_{10}^A , the angular velocity $\omega_{10}^A = \dot{\varphi}_{10}^A$ and the angular acceleration $\varepsilon_{10}^A = \ddot{\varphi}_{10}^A$.

A prismatic joint is as well as a piston linked at the $A_2x_2^A y_2^A z_2^A$ frame, having a relative motion with the displacement λ_{21}^A , the velocity $v_{21}^A = \dot{\lambda}_{21}^A$ and the acceleration $\gamma_{21}^A = \ddot{\lambda}_{21}^A$. It has the length l_2 , mass m_2^A and tensor of inertia \hat{J}_2^A . A new revolute joint is introduced at a homogenous rod of length h , mass m_3^A and tensor of inertia \hat{J}_3^A , linked at the $A_3x_3^A y_3^A z_3^A$ frame, having a perpendicular rotation about z_3^A axis with the angle ϕ_{32}^A , the angular velocity $\omega_{32}^A = \dot{\phi}_{32}^A$ and the angular acceleration $\varepsilon_{32}^A = \ddot{\phi}_{32}^A$. Finally, the median axis of the moving platform of mass m_4^A and tensor of inertia \hat{J}_4^A rotates around the rod A_3G with the angle ϕ_{43}^A , the angular velocity $\omega_{43}^A = \dot{\phi}_{43}^A$ and the angular acceleration $\varepsilon_{43}^A = \ddot{\phi}_{43}^A$.

Concerning other two active kinematical chains, the architecture of the leg B , for example, consists of the cross of a fixed Hooke joint characterised by a negligible mass, linked at the frame $B_1x_1^B y_1^B z_1^B$, which has the angle of rotation ϕ_{10}^B , the absolute angular velocity $\omega_{10}^B = \dot{\phi}_{10}^B$ and the angular acceleration $\varepsilon_{10}^B = \ddot{\phi}_{10}^B$. This is connected at a moving cylinder $B_2x_2^B y_2^B z_2^B$ of length l_3 , mass m_2^B and tensor of inertia \hat{J}_2^B , having a relative rotation around $B_2z_2^B$ axis with the angle ϕ_{21}^B , so that $\omega_{21}^B = \dot{\phi}_{21}^B$, $\varepsilon_{21}^B = \ddot{\phi}_{21}^B$. An actuated prismatic joint is as well as a piston of length l_4 , mass m_3^B and tensor of inertia \hat{J}_3^B , linked to the $B_3x_3^B y_3^B z_3^B$ frame, having a relative displacement λ_{32}^B , the velocity $v_{32}^B = \dot{\lambda}_{32}^B$ and the acceleration $\gamma_{32}^B = \ddot{\lambda}_{32}^B$. Finally, a second universal joint B_4 is introduced at the apex of the rectangular moving platform.

Additionally, two rigid cranks of lengths l_5, l_6 , masses m_1^D, m_1^E and tensors of inertia \hat{J}_1^D, \hat{J}_1^E , respectively, jointed at two fixed revolute pairs D_1, E_1 , execute oscillating rotations with the angles ϕ_{10}^D, ϕ_{10}^E , the angular velocities $\omega_{10}^D, \omega_{10}^E$ and the angular accelerations $\varepsilon_{10}^D, \varepsilon_{10}^E$. Finally, the internal prismatic pair E_2 of negligible mass starts from an initial position $D_2E_2 = s$ and has the relative displacement λ , the velocity $v = \dot{\lambda}$ and the acceleration $\gamma = \ddot{\lambda}$.

Starting from the reference origin O and pursuing along five independent legs $OA_1A_2A_3A_4, OB_1B_2B_3, OC_1C_2C_3, OD_1, OE_1$, we obtain following transformation matrices

$$\begin{aligned}
a_{10} &= a_{10}^{\phi} a_1^{\alpha}, \quad a_{21} = \theta, \quad a_{32} = a_{32}^{\phi} a_2^{\alpha} \theta, \quad a_{43} = a_{43}^{\phi} \theta^{\text{T}}, \\
b_{10} &= b_{10}^{\phi}, \quad b_{21} = b_{21}^{\phi} a_3^{\alpha} \theta, \quad b_{32} = \theta, \\
c_{10} &= c_{10}^{\phi}, \quad c_{21} = c_{21}^{\phi} a_3^{\alpha} \theta^{\text{T}}, \quad c_{32} = \theta, \quad d_{10} = d_{10}^{\phi} a_4^{\alpha}, \quad e_{10} = e_{10}^{\phi} a_5^{\alpha},
\end{aligned} \tag{1}$$

where we denote the matrices:

$$a_i^{\alpha} = \text{rot}(z, \alpha_i), \quad \theta = \text{rot}(y, \frac{\pi}{2}), \quad p_{k,k-1}^{\phi} = \text{rot}(z, \phi_{k,k-1}) \quad (p = a, b, c, d, e). \tag{2}$$

A complete description of the absolute position and orientation of the platform requires four variables: the coordinates x_0^G, y_0^G of the point G and two Euler's angles ψ, ϕ associated with two successive orthogonal rotations. Since all rotations take place successively about the moving coordinate axes, the general rotation matrix $R = R_{21}R_{10}$ is obtained by multiplying two known transformation matrices

$$R_{10} = \text{rot}(z, \psi + \alpha_1 - \alpha_2), \quad R_{21} = \text{rot}(x, \phi). \tag{3}$$

Here, x_0^G, y_0^G and ϕ are chosen as the independent variables and ψ is a parameter of a *parasitic* motion. The parasitic motion from the four motions of the moving platform is permanently dependent on the independent variables.

The conditions concerning the absolute orientation of the moving platform are given by the following matrix identity

$$\theta^{\text{T}} a_{40} = R, \tag{4}$$

from which we obtain significant relations between the angles of rotation

$$\psi = \phi_{10}^A - \phi_{32}^A, \quad \phi = \phi_{43}^A. \tag{5}$$

In the inverse geometric problem, the position of the mechanism is completely given through three variables x_0^G, y_0^G, ϕ . For the parallel simulator, the rotation angle ϕ is the only *completely independent* variable with other three pose parameters.

Consider, for example, that during three seconds the rotation of the moving platform around its median axis and the motion of the characteristic point G along a *rectilinear trajectory* are expressed in the fixed frame $Ox_0y_0z_0$ through the following analytical functions

$$\frac{x_0^G - (d_2 + d_3 + d_4)}{x_0^{G*}} = \frac{y_0^G - h_G}{y_0^{G*}} = \frac{\phi}{\phi^*} = 1 - \cos \frac{\pi}{3} t, \tag{6}$$

where the values $2x_0^{G^*}, 2y_0^{G^*}, 2\phi^*$ denote the final position and orientation of the moving platform.

A set of 12 independent variables $\varphi_{10}^A, \lambda_{21}^A, \varphi_{32}^A, \varphi_{10}^B, \varphi_{21}^B, \lambda_{32}^B, \varphi_{10}^C, \varphi_{21}^C, \lambda_{32}^C, \varphi_{10}^D, \varphi_{10}^E, \lambda$ will be determined by vector-loop equations

$$\begin{aligned} \vec{r}_{10}^A + \sum_{k=1}^3 a_{k0}^T \vec{r}_{k+1,k}^A + a_{40}^T \vec{r}_4^G &= \vec{r}_{10}^B + \sum_{k=1}^2 b_{k0}^T \vec{r}_{k+1,k}^B + b_{30}^T \vec{r}_3^{B_4} - a_{40}^T \vec{r}_4^{GB_4} = \\ &= \vec{r}_{10}^C + \sum_{k=1}^2 c_{k0}^T \vec{r}_{k+1,k}^C + c_{30}^T \vec{r}_3^{C_4} - a_{40}^T \vec{r}_4^{GC_4} = \vec{r}_{10}^D + d_{10}^T \vec{r}_1^{D_2} + a_{30}^T \vec{r}_3^{D_2G} = \\ &= \vec{r}_{10}^E + e_{10}^T \vec{r}_1^{E_2} + a_{30}^T \vec{r}_3^{E_2G} = \vec{r}_0^G, \end{aligned} \quad (7)$$

where

$$\begin{aligned} \vec{r}_{10}^A &= \vec{0}, \quad \vec{r}_{21}^A = (s_A + \lambda_{21}^A) \vec{u}_1, \quad \vec{r}_{32}^A = l_2 \vec{u}_3, \quad \vec{r}_{43}^A = \vec{0}, \quad \vec{r}_4^G = h \vec{u}_3 \\ \vec{r}_{10}^B &= [d_2 + d_3 + d_4 \quad 0 \quad d_5]^T, \quad \vec{r}_{21}^B = \vec{0}, \quad \vec{r}_{32}^B = (s_B + \lambda_{32}^B) \vec{u}_1, \quad \vec{r}_3^{B_4} = l_4 \vec{u}_3, \quad \vec{r}_4^{GB_4} = -\frac{1}{2} b \vec{u}_1 \\ \vec{r}_{10}^C &= [d_2 + d_3 + d_4 \quad 0 \quad -d_5]^T, \quad \vec{r}_{21}^C = \vec{0}, \quad \vec{r}_{32}^C = (s_C + \lambda_{32}^C) \vec{u}_1, \quad \vec{r}_3^{C_4} = l_4 \vec{u}_3, \quad \vec{r}_4^{GC_4} = \frac{1}{2} b \vec{u}_1 \\ \vec{r}_{10}^D &= (d_2 + d_3) \vec{u}_1, \quad \vec{r}_1^{D_2} = l_5 \vec{u}_1, \quad \vec{r}_3^{D_2G} = (d_1 - h) \vec{u}_1 \\ \vec{r}_{10}^E &= d_2 \vec{u}_1, \quad \vec{r}_1^{E_2} = l_6 \vec{u}_1, \quad \vec{r}_3^{E_2G} = (s + d_1 - h + \lambda) \vec{u}_1 \\ \vec{u}_1 &= [1 \quad 0 \quad 0]^T, \quad \vec{u}_3 = [0 \quad 0 \quad 1]^T. \end{aligned} \quad (8)$$

From the vector equations (7) we obtain 12 analytical equations for the inverse geometric solution, giving the expressions of all 12 above independent variables.

The motions of the component elements of the manipulator are characterized by the relative velocities of the joints

$$\vec{v}_{k,k-1} = \dot{\lambda}_{k,k-1} \vec{u}_3 \quad (9)$$

or by the relative angular velocities and their *associated* skew-symmetric matrices

$$\vec{\omega}_{k,k-1} = \dot{\phi}_{k,k-1} \vec{u}_3, \quad \tilde{\omega}_{k,k-1} = \dot{\phi}_{k,k-1} \tilde{u}_3. \quad (10)$$

Deriving the relations (5) and the geometrical constraints (7), we obtain first the angular velocity $\omega_{43}^A = \dot{\phi}$ and 12 *matrix conditions of connectivity* [12]:

$$\vec{V} = [Q]^{-1} \vec{P}, \quad (11)$$

where followings nonzero terms determines the contents of 12×12 invertible square matrix $[Q]$ and the column matrix \vec{P} :

$$\begin{aligned} q_{i1}^A &= \vec{u}_i^T a_{10}^T \tilde{u}_3 \{ \vec{r}_{21}^A + a_{21}^T \vec{r}_{32}^A + a_{21}^T a_{32}^T a_{43}^T \vec{r}_4^G \}, & q_{i2}^A &= \vec{u}_i^T a_{10}^T \vec{u}_1, & q_{i3}^A &= \vec{u}_i^T a_{30}^T \tilde{u}_3 a_{43}^T \vec{r}_4^G \\ q_{j1}^B &= -\vec{u}_j^T a_{10}^T \tilde{u}_3 a_{21}^T a_{32}^T a_{43}^T \vec{r}_4^{GB_4}, & q_{j3}^B &= -\vec{u}_j^T a_{30}^T \tilde{u}_3 a_{43}^T \vec{r}_4^{GB_4}, \\ q_{j4}^B &= \vec{u}_j^T b_{10}^T \tilde{u}_3 b_{21}^T \{ \vec{r}_{32}^B + b_{32}^T \vec{r}_3^{B_4} \}, & q_{j5}^B &= \vec{u}_j^T b_{20}^T \tilde{u}_3 \{ \vec{r}_{32}^B + b_{32}^T \vec{r}_3^{B_4} \}, & q_{j6}^B &= \vec{u}_j^T b_{20}^T \vec{u}_1 \\ q_{j1}^C &= -\vec{u}_j^T a_{10}^T \tilde{u}_3 a_{21}^T a_{32}^T a_{43}^T \vec{r}_4^{GC_4}, & q_{j3}^C &= -\vec{u}_j^T a_{30}^T \tilde{u}_3 a_{43}^T \vec{r}_4^{GC_4}, \\ q_{j7}^C &= \vec{u}_j^T c_{10}^T \tilde{u}_3 c_{21}^T \{ \vec{r}_{32}^C + c_{32}^T \vec{r}_3^{C_4} \}, & q_{j8}^C &= \vec{u}_j^T c_{20}^T \tilde{u}_3 \{ \vec{r}_{32}^C + c_{32}^T \vec{r}_3^{C_4} \}, & q_{j9}^C &= \vec{u}_j^T c_{20}^T \vec{u}_1 \\ q_{i1}^D &= \vec{u}_i^T a_{10}^T \tilde{u}_3 a_{21}^T a_{32}^T \vec{r}_3^{D_2G}, & q_{i3}^D &= \vec{u}_i^T a_{30}^T \tilde{u}_3 \vec{r}_3^{D_2G}, & q_{i10}^D &= \vec{u}_i^T d_{10}^T \tilde{u}_3 \vec{r}_1^{D_2} \\ q_{i1}^E &= \vec{u}_i^T a_{10}^T \tilde{u}_3 a_{21}^T a_{32}^T \vec{r}_3^{E_2G}, & q_{i3}^E &= \vec{u}_i^T a_{30}^T \tilde{u}_3 \vec{r}_3^{E_2G}, & q_{i11}^E &= \vec{u}_i^T e_{10}^T \tilde{u}_3 \vec{r}_1^{E_2}, & q_{i12}^E &= \vec{u}_i^T a_{30}^T \vec{u}_1 \\ p_i^A &= \vec{u}_i^T \dot{\vec{r}}_0^G, & p_j^B &= \vec{u}_j^T \dot{\vec{r}}_0^G + \dot{\phi} \vec{u}_j^T a_{40}^T \tilde{u}_3 \vec{r}_4^{GB_4}, & p_j^C &= \vec{u}_j^T \dot{\vec{r}}_0^G + \dot{\phi} \vec{u}_j^T a_{40}^T \tilde{u}_3 \vec{r}_4^{GC_4} \\ p_i^D &= \vec{u}_i^T \dot{\vec{r}}_0^G, & p_i^E &= \vec{u}_i^T \dot{\vec{r}}_0^G & & (i = 1, 2; j = 1, 2, 3). \end{aligned} \quad (12)$$

Finally, the expressions of relative velocities are obtained from the column matrix

$$\vec{V} = [\omega_{10}^A \ v_{21}^A \ \omega_{32}^A \ \omega_{10}^B \ \omega_{21}^B \ v_{32}^B \ \omega_{10}^C \ \omega_{21}^C \ v_{32}^C \ \omega_{10}^D \ \omega_{10}^E \ v]^T. \quad (13)$$

Considering some independent *virtual motions* of the spatial mechanism, virtual displacements and velocities should be compatible with the virtual motions imposed by all kinematical constraints and joints at a given instant in time. Let us assume that the robot has successively three virtual motions determined by following sets of velocities:

$$\begin{aligned} v_{21a}^{Av} &= 1, v_{32a}^{Bv} = 0, v_{32a}^{Cv} = 0 \\ v_{21b}^{Av} &= 0, v_{32b}^{Bv} = 1, v_{32b}^{Cv} = 0 \\ v_{21c}^{Av} &= 0, v_{32c}^{Bv} = 0, v_{32c}^{Cv} = 1. \end{aligned} \quad (14)$$

The characteristic *virtual velocities* are expressed as functions of the pose of the mechanism by the general kinematical equations (11).

Expressions of relative accelerations are obtained from the column matrix

$$\vec{\Gamma} = [\varepsilon_{10}^A \quad \gamma_{21}^A \quad \varepsilon_{32}^A \quad \varepsilon_{10}^B \quad \varepsilon_{21}^B \quad \gamma_{32}^B \quad \varepsilon_{10}^C \quad \varepsilon_{21}^C \quad \gamma_{32}^C \quad \varepsilon_{10}^D \quad \varepsilon_{10}^E \quad \gamma]^T. \quad (15)$$

using new conditions of connectivity:

$$\vec{\Gamma} = [Q]^{-1} \vec{S}, \quad (16)$$

where following terms determine the contents of column matrix $\vec{S} = \dot{\vec{P}} - [\dot{Q}] \vec{V}$:

$$s_i^A = \ddot{u}_i^T \vec{r}_0^G - \omega_{10}^A \omega_{10}^A \vec{u}_i^T a_{10}^T \tilde{u}_3 \tilde{u}_3 \{ \vec{r}_{21}^A + a_{21}^T \vec{r}_{32}^A + a_{21}^T a_{32}^T a_{43}^T \vec{r}_4^G \} - \omega_{32}^A \omega_{32}^A \vec{u}_i^T a_{30}^T \tilde{u}_3 \tilde{u}_3 a_{43}^T \vec{r}_4^G - 2\omega_{10}^A v_{21}^T \vec{u}_i^T a_{10}^T \tilde{u}_3 \vec{u}_1 - 2\omega_{10}^A \omega_{32}^A \vec{u}_i^T a_{10}^T \tilde{u}_3 a_{21}^T a_{32}^T \tilde{u}_3 a_{43}^T \vec{r}_4^G \}$$

$$s_j^B = \ddot{u}_j^T \vec{r}_0^G + \ddot{\phi} \vec{u}_j^T a_{40}^T \tilde{u}_3 \vec{r}_4^{GB_4} + \omega_{10}^A \omega_{10}^A \vec{u}_j^T a_{10}^T \tilde{u}_3 \tilde{u}_3 a_{21}^T a_{32}^T a_{43}^T \vec{r}_4^{GB_4} + \omega_{32}^A \omega_{32}^A \vec{u}_j^T a_{30}^T \tilde{u}_3 \tilde{u}_3 a_{43}^T \vec{r}_4^{GB_4} + \dot{\phi}^2 \vec{u}_j^T a_{40}^T \tilde{u}_3 \tilde{u}_3 \vec{r}_4^{GB_4} + 2\omega_{10}^A \omega_{32}^A \vec{u}_j^T a_{10}^T \tilde{u}_3 a_{21}^T a_{32}^T \tilde{u}_3 a_{43}^T \vec{r}_4^{GB_4} + 2\omega_{10}^A \dot{\phi} \vec{u}_j^T a_{10}^T \tilde{u}_3 a_{21}^T a_{32}^T a_{43}^T \tilde{u}_3 \vec{r}_4^{GB_4} + 2\omega_{32}^A \dot{\phi} \vec{u}_j^T a_{30}^T \tilde{u}_3 a_{43}^T \tilde{u}_3 \vec{r}_4^{GB_4} - \omega_{10}^B \omega_{10}^B \vec{u}_j^T b_{10}^T \tilde{u}_3 \tilde{u}_3 b_{21}^T \{ \vec{r}_{32}^B + b_{32}^T \vec{r}_3^B \} - \omega_{21}^B \omega_{21}^B \vec{u}_j^T b_{20}^T \tilde{u}_3 \tilde{u}_3 \{ \vec{r}_{32}^B + b_{32}^T \vec{r}_3^B \} - 2\omega_{10}^B \omega_{21}^B \vec{u}_j^T b_{10}^T \tilde{u}_3 b_{21}^T \tilde{u}_3 \{ \vec{r}_{32}^B + b_{32}^T \vec{r}_3^B \} - 2\omega_{10}^B v_{32}^T \vec{u}_j^T b_{10}^T \tilde{u}_3 b_{21}^T \vec{u}_1 - 2\omega_{21}^B v_{32}^T \vec{u}_j^T b_{20}^T \tilde{u}_3 \vec{u}_1$$

$$s_j^C = \ddot{u}_j^T \vec{r}_0^G + \ddot{\phi} \vec{u}_j^T a_{40}^T \tilde{u}_3 \vec{r}_4^{GC_4} + \omega_{10}^A \omega_{10}^A \vec{u}_j^T a_{10}^T \tilde{u}_3 \tilde{u}_3 a_{21}^T a_{32}^T a_{43}^T \vec{r}_4^{GC_4} + \omega_{32}^A \omega_{32}^A \vec{u}_j^T a_{30}^T \tilde{u}_3 \tilde{u}_3 a_{43}^T \vec{r}_4^{GC_4} + \dot{\phi}^2 \vec{u}_j^T a_{40}^T \tilde{u}_3 \tilde{u}_3 \vec{r}_4^{GC_4} + 2\omega_{10}^A \omega_{32}^A \vec{u}_j^T a_{10}^T \tilde{u}_3 a_{21}^T a_{32}^T \tilde{u}_3 a_{43}^T \vec{r}_4^{GC_4} + 2\omega_{10}^A \dot{\phi} \vec{u}_j^T a_{10}^T \tilde{u}_3 a_{21}^T a_{32}^T a_{43}^T \tilde{u}_3 \vec{r}_4^{GC_4} + 2\omega_{32}^A \dot{\phi} \vec{u}_j^T a_{30}^T \tilde{u}_3 a_{43}^T \tilde{u}_3 \vec{r}_4^{GC_4} - \omega_{10}^C \omega_{10}^C \vec{u}_j^T c_{10}^T \tilde{u}_3 \tilde{u}_3 c_{21}^T \{ \vec{r}_{32}^C + c_{32}^T \vec{r}_3^C \} - \omega_{21}^C \omega_{21}^C \vec{u}_j^T c_{20}^T \tilde{u}_3 \tilde{u}_3 \{ \vec{r}_{32}^C + c_{32}^T \vec{r}_3^C \} - 2\omega_{10}^C \omega_{21}^C \vec{u}_j^T c_{10}^T \tilde{u}_3 c_{21}^T \tilde{u}_3 \{ \vec{r}_{32}^C + c_{32}^T \vec{r}_3^C \} - 2\omega_{10}^C v_{32}^T \vec{u}_j^T c_{10}^T \tilde{u}_3 c_{21}^T \vec{u}_1 - 2\omega_{21}^C v_{32}^T \vec{u}_j^T c_{20}^T \tilde{u}_3 \vec{u}_1$$

$$s_i^D = \ddot{u}_i^T \vec{r}_0^G - \omega_{10}^A \omega_{10}^A \vec{u}_i^T a_{10}^T \tilde{u}_3 \tilde{u}_3 a_{21}^T a_{32}^T \vec{r}_3^{D_2G} - \omega_{32}^A \omega_{32}^A \vec{u}_i^T a_{30}^T \tilde{u}_3 \tilde{u}_3 \vec{r}_3^{D_2G} - \omega_{10}^D \omega_{10}^D \vec{u}_i^T d_{10}^T \tilde{u}_3 \tilde{u}_3 \vec{r}_1^{D_2} - 2\omega_{10}^A \omega_{32}^A \vec{u}_i^T a_{10}^T \tilde{u}_3 a_{21}^T a_{32}^T \tilde{u}_3 \vec{r}_3^{D_2G}$$

$$\begin{aligned}
s_i^E = & \vec{u}_j^T \ddot{\vec{r}}_0^G - \omega_{10}^A \omega_{10}^A \vec{u}_i^T a_{10}^T \tilde{u}_3 \tilde{u}_3 a_{21}^T a_{32}^T \vec{r}_3^{E_2G} - \omega_{32}^A \omega_{32}^A \vec{u}_i^T a_{30}^T \tilde{u}_3 \tilde{u}_3 \vec{r}_3^{E_2G} - \\
& - \omega_{10}^E \omega_{10}^E \vec{u}_i^T e_{10}^T \tilde{u}_3 \tilde{u}_3 \vec{r}_1^{E_2} - 2\omega_{10}^A \omega_{32}^A \vec{u}_i^T a_{10}^T \tilde{u}_3 a_{21}^T a_{32}^T \tilde{u}_3 \vec{r}_3^{E_2G} - \\
& - 2\omega_{10}^A v \vec{u}_i^T a_{10}^T \tilde{u}_3 a_{21}^T a_{32}^T \vec{u}_1 - -2\omega_{32}^A v \vec{u}_i^T a_{30}^T \tilde{u}_3 \vec{u}_1
\end{aligned}$$

($i = 1, 2 ; j = 1, 2, 3$).

(17)

3. INVERSE DYNAMICS MODEL

The dynamics analysis of parallel robots is complicated because the existence of a spatial kinematical structure, which possesses a large number of passive degrees of freedom, dominance of the inertial forces, frictional and gravitational components and by the problem linked to real-time control in the inverse dynamics. Considering all gravitational effects and neglecting the frictions forces, the relevant objective of the inverse dynamics is to determine the input torques or forces, which must be exerted by the actuators in order to produce a given trajectory of the end-effector.

A lot of works have focused on the dynamics of Stewart platform. Dasgupta and Mruthyunjaya [13] used the Newton-Euler approach to develop closed-form dynamic equations of Stewart platform, considering all dynamic and gravity effects as well as viscous friction at joints. Tsai and Stamper [14] presented an algorithm to solve the inverse dynamics for the Delta translational robot, using Newton-Euler equations and Lagrange formalism.

Three independent pneumatic or hydraulic systems A, B, C that generate three input forces $\vec{f}_{21}^A = f_{21}^A \vec{u}_3$, $\vec{f}_{32}^B = f_{32}^B \vec{u}_3$, $\vec{f}_{32}^C = f_{32}^C \vec{u}_3$, which are oriented along the axes $A_2 z_2^A, B_3 z_3^B, C_3 z_3^C$, control the motion of three moving pistons of the legs.

The parallel robot can artificially be transformed in a set of three open chains C_i ($i = A, B, C$) subject to the constraints. This is possible by cutting each joint for moving platform and taking its effect into account by introducing the corresponding constraint conditions.

The force of inertia and the resulting moment of inertia forces of a rigid body T_k^A , for example,

$$\begin{aligned}
\vec{F}_{k0}^{inA} = & -m_k^A \left[\vec{\gamma}_{k0}^A + \left(\tilde{\omega}_{k0}^A \tilde{\omega}_{k0}^A + \tilde{\varepsilon}_{k0}^A \right) \vec{r}_k^{CA} \right], \\
\vec{M}_{k0}^{inA} = & -[m_k^A \tilde{r}_k^{CA} \vec{\gamma}_{k0}^A + \hat{J}_k^{A \rightarrow A} \tilde{\varepsilon}_{k0}^A + \tilde{\omega}_{k0}^A \hat{J}_k^{A \rightarrow A} \tilde{\omega}_{k0}^A],
\end{aligned}$$
(18)

are determined with respect to the centre of joint A_k . On the other hand, the wrench of two vectors \vec{F}_k^{*A} and \vec{M}_k^{*A} evaluates the influence of the action of the weight $m_k^A \vec{g}$ and of other external and internal forces applied to the same element T_k^A of the manipulator, for example:

$$\vec{F}_k^{*A} = m_k^A g a_{k0} \vec{u}_3, \quad \vec{M}_k^{*A} = m_k^A g \tilde{r}_k^{CA} a_{k0} \vec{u}_3 \quad (k=1,2,3,4). \quad (19)$$

Pursuing the first leg A , two recursive relations generate the vectors

$$\vec{F}_k^A = \vec{F}_{k0}^A + a_{k+1,k}^T \vec{F}_{k+1}^A, \quad \vec{M}_k^A = \vec{M}_{k0}^A + a_{k+1,k}^T \vec{M}_{k+1}^A + \tilde{r}_{k+1,k}^A a_{k+1,k}^T \vec{F}_{k+1}^A, \quad (20)$$

where one denoted

$$\vec{F}_{k0}^A = -\vec{F}_k^{inA} - \vec{F}_k^{*A}, \quad \vec{M}_{k0}^A = -\vec{M}_k^{inA} - \vec{M}_k^{*A}. \quad (21)$$

As example, starting from (20), we develop a set of recursive relations:

$$\begin{aligned} \vec{F}_4^A &= \vec{F}_{40}^A, \quad \vec{F}_3^A = \vec{F}_{30}^A + a_{43}^T \vec{F}_4^A, \quad \vec{F}_2^A = \vec{F}_{20}^A + a_{32}^T \vec{F}_3^A, \quad \vec{F}_1^A = \vec{F}_{10}^A + a_{21}^T \vec{F}_2^A \\ \vec{M}_4^A &= \vec{M}_{40}^A, \quad \vec{M}_3^A = \vec{M}_{30}^A + a_{43}^T \vec{M}_4^A + \tilde{r}_{43}^A a_{43}^T \vec{F}_4^A \\ \vec{M}_2^A &= \vec{M}_{20}^A + a_{32}^T \vec{M}_3^A + \tilde{r}_{32}^A a_{32}^T \vec{F}_3^A, \quad \vec{M}_1^A = \vec{M}_{10}^A + a_{21}^T \vec{M}_2^A + \tilde{r}_{21}^A a_{21}^T \vec{F}_2^A. \end{aligned} \quad (22)$$

The fundamental principle of the virtual work states that a mechanism is under dynamic equilibrium if and only if the total virtual work developed by all external, internal and inertia forces vanish during any general virtual displacement, which is compatible with the constraints imposed on the mechanism.

Applying the explicit form of *equations of the parallel robots dynamics* [15], compact matrix relations result for the input force of three *prismatic actuators*

$$\begin{aligned} f_{21}^A &= \vec{u}_3^T \{ \vec{F}_2^A + \omega_{10a}^{Av} \vec{M}_1^A + \omega_{32a}^{Av} \vec{M}_3^A + \omega_{43a}^{Av} \vec{M}_4^A + \omega_{10a}^{Bv} \vec{M}_1^B + \\ &\quad + \omega_{21a}^{Bv} \vec{M}_2^B + \omega_{10a}^{Cv} \vec{M}_1^C + \omega_{21a}^{Cv} \vec{M}_2^C + \omega_{10a}^{Dv} \vec{M}_1^D + \omega_{10a}^{Ev} \vec{M}_1^E \} \\ f_{32}^B &= \vec{u}_3^T \{ \vec{F}_3^B + \omega_{10b}^{Bv} \vec{M}_1^B + \omega_{21b}^{Bv} \vec{M}_2^B + \omega_{10b}^{Cv} \vec{M}_1^C + \omega_{21b}^{Cv} \vec{M}_2^C + \\ &\quad + \omega_{10b}^{Av} \vec{M}_1^A + \omega_{32a}^{Av} \vec{M}_3^A + \omega_{43b}^{Av} \vec{M}_4^A + \omega_{10b}^{Dv} \vec{M}_1^D + \omega_{10a}^{Ev} \vec{M}_1^E \} \\ f_{32}^C &= \vec{u}_3^T \{ \vec{F}_3^C + \omega_{10c}^{Cv} \vec{M}_1^C + \omega_{21c}^{Cv} \vec{M}_2^C + \omega_{10c}^{Bv} \vec{M}_1^B + \omega_{21c}^{Bv} \vec{M}_2^B + \\ &\quad + \omega_{10c}^{Av} \vec{M}_1^A + \omega_{32c}^{Av} \vec{M}_3^A + \omega_{43c}^{Av} \vec{M}_4^A + \omega_{10c}^{Dv} \vec{M}_1^D + \omega_{10c}^{Ev} \vec{M}_1^E \}. \end{aligned} \quad (23)$$

The relations (20)–(23) represent the *inverse dynamics model* of the parallel flight simulator. The various dynamical effects, including the Coriolis and

centrifugal forces coupling and the gravitational actions are considered in this explicit equation.

As an application let us consider a parallel simulator which has the following geometrical and architectural characteristics

$$x_0^{G^*} = 0.05 \text{ m}, \quad y_0^{G^*} = 0.1 \text{ m}, \quad \phi^* = \pi/12$$

$$A_3D_2 = d_1 = 0.4 \text{ m}, \quad A_1E_1 = d_2 = 0.95 \text{ m}, \quad E_1D_1 = d_3 = 0.65 \text{ m}$$

$$D_1F = d_4 = 0.25 \text{ m}, \quad B_2F = C_2F = d_5 = 1.35 \text{ m}$$

$$D_1D_2 = l_5 = 1.3 \text{ m}, \quad E_1E_2 = l_6 = 1.2 \text{ m}, \quad B_4C_4 = b = 1.2 \text{ m}$$

$$A_4G = h = 1.4 \text{ m}, \quad FG = h_G = 1.1 \text{ m}, \quad \Delta t = 3 \text{ s}$$

$$s_A = 0.29 \text{ m}, \quad s_B = s_C = 0.33 \text{ m}$$

$$l_1 = 0.65 \text{ m}, \quad l_2 = 0.85 \text{ m}, \quad l_3 = 0.75 \text{ m}, \quad l_4 = 1 \text{ m}$$

$$m_1^A = 1 \text{ kg}, \quad m_2^A = 1.2 \text{ kg}, \quad m_3^A = 1.5 \text{ kg}, \quad m_4^A = 5 \text{ kg}$$

$$m_2^B = m_2^C = 1 \text{ kg}, \quad m_3^B = m_3^C = 1.2 \text{ kg}, \quad m_1^D = 1.5 \text{ kg}, \quad m_1^E = 1.4 \text{ kg}.$$

Using MATLAB software, a computer program was developed to solve the dynamics of the parallel simulator. To develop the algorithm, it is assumed that the platform starts at rest from a central configuration and moves pursuing successively some evolutions.

Three examples are solved to illustrate the algorithm. In a first example, the platform's point G moves along the *vertical direction* Oy_0 with variable acceleration while all the other positional parameters are held equal to zero. As can be seen from Fig.3 and Fig.4 it is proved to be true that the active forces and powers of the actuators B and C are permanently equal to one another.

For the case when the point G moves along a *rectilinear trajectory* without a rotation of the platform around its median axis, the graphs are illustrated in Fig.5 and Fig. 6.

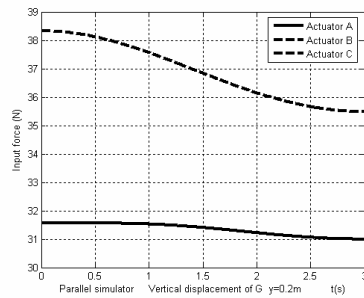


Fig. 3 – Input forces of three actuators.

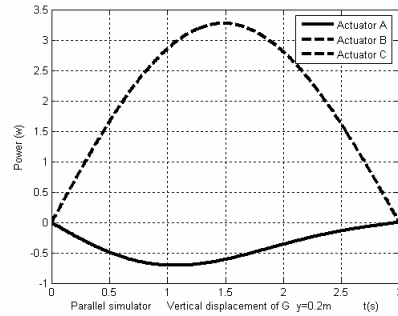


Fig. 4 – Powers of three actuators.

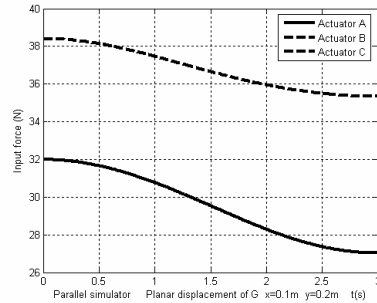


Fig. 5 – Input forces of three actuators.

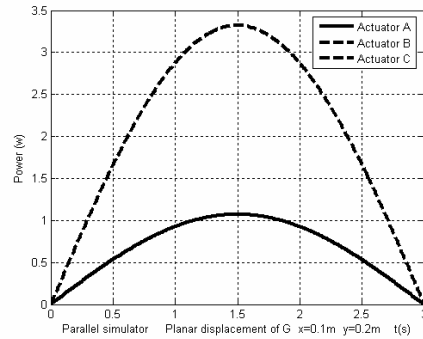


Fig. 6 – Powers of three actuators.

Further on, we shall consider a *general evolution* of the platform, combining a rectilinear displacement of the point G and a rotation of the platform around its median axis. The input forces and powers of three prismatic actuators are graphically sketched in Fig. 7 and Fig. 8.

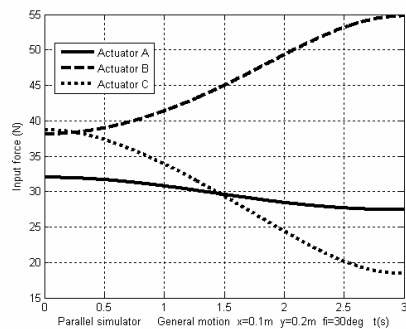


Fig. 7 – Input forces of three actuators.

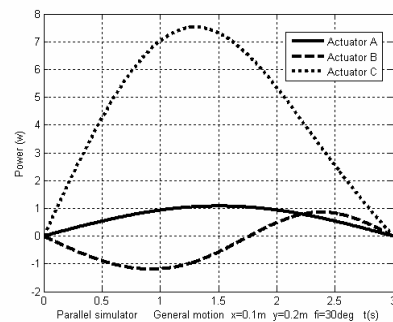


Fig. 8 – Powers of three actuators.

4. CONCLUSIONS

Some exact relations that give in real-time the position, velocity and acceleration of each element of a flight parallel simulator have been established in the present paper. The dynamics models take into consideration the masses and forces of inertia introduced by all component elements of the parallel mechanism. Based on explicit equations of parallel robots dynamics, the approach can eliminate all forces of internal joints and establishes a direct determination of the time-history evolution of active forces and powers required by the actuators.

The simulation certifies that one of the major advantages of the current matrix recursive formulation is the accuracy and a smaller processing time for the numerical computation. Choosing the appropriate serial kinematical circuits connecting many moving platforms, the present method can be easily applied in forward and inverse mechanics of various types of parallel mechanisms, complex manipulators of higher degrees of freedom and particularly *hybrid structures*, with increased number of components of the mechanisms.

Received on December 2, 2013

REFERENCES

1. TSAI, L-W., *Robot analysis: the mechanics of serial and parallel manipulators*, Wiley, 1999.
2. PLITEA, N., LESE, D., PISLA, D., VAIDA, C., *Structural design and kinematics of a new parallel reconfigurable robot*, Robotics and Computer-Integrated Manufacturing, **29**, 1, pp. 219–235, 2013.
3. PISLA, D., ITUL, T., PISLA, A., GHERMAN, B., *Dynamics of a Parallel Platform for Helicopter Flight Simulation Considering Friction*, SYROM 2009, Springer, 2009, pp. 365–378.
4. MERLET, J-P., *Parallel robots*, Kluwer Academic, 2000.
5. G. GOGU, *T2R1-type parallel manipulators with bifurcated planar-spatial motion*, European Journal of Mechanics, A/Solids, **33**, pp. 1–11, 2012.
6. STEWART, D., *A Platform with Six Degrees of Freedom*, Proc. Inst. Mech. Eng., **180**, 1, pp. 371–386, 1965.
7. DI GREGORIO, R., PARENTI CASTELLI, V., *Dynamics of a class of parallel wrists*, ASME Journal of Mechanical Design, **126**, 3, pp. 436–441, 2004.
8. PISLA, A., ITUL, T., PISLA, D., SZILAGHYI, A., *Considerations upon the influence of manufacturing and assembly errors on the kinematic and dynamic behavior in a flight simulator Stewart-Gough platform*, Mechanisms, Transmissions and Applications: Mechanisms and Machine Science, **3**, Springer, 2012, pp. 215–223.
9. GWINNETT, J.E., *Amusement devices*, US Patent No. 1789680, 1931.
10. GALANOV, A.S., DIACIUN, V.C., *Manipulator*, URSS Patent No. 908589, 1982.
11. ANGELES, J., *Fundamentals of Robotic Mechanical Systems: Theory, Methods and Algorithms*, Springer, 2002.
12. STAICU, S., *Méthodes matricielles en cinématique des mécanismes*, UPB Scientific Bulletin, Series D: Mechanical Engineering, **62**, 1, pp. 3–10, 2000.
13. DASGUPTA, B., MRUTHYUNJAYA, T.S., *A Newton-Euler formulation for the inverse dynamics of the Stewart platform manipulator*, Mechanism and Machine Theory, **34**, pp. 711–725, 1998.
14. TSAI, L-W., STAMPER, R., *A parallel manipulator with only translational degrees of freedom*, ASME Design Engineering Technical Conferences, Irvine, CA, 1996.
15. STAICU, S., LIU, X-J., LI, J., *Explicit dynamics equations of the constrained robotic systems*, Nonlinear Dynamics, **58**, 1–2, pp. 217–235, 2009.